



## **Integrity of clay till aquitards to DNAPL migration: Assessment using current and emerging characterization tools**

**Fjordbøge, Annika Sidelmann; Janniche, Gry Sander; Jørgensen, Torben H.; Groesen, Bernt; Wealthall, Gary; Christensen, Anders G.; Kern-Jespersen, Henriette; Broholm, Mette Martina**

*Published in:*  
Ground Water Monitoring & Remediation

*Link to article, DOI:*  
[10.1111/gwmr.12217](https://doi.org/10.1111/gwmr.12217)

*Publication date:*  
2017

*Document Version*  
Peer reviewed version

[Link back to DTU Orbit](#)

*Citation (APA):*  
Fjordbøge, A. S., Janniche, G. S., Jørgensen, T. H., Groesen, B., Wealthall, G., Christensen, A. G., Kern-Jespersen, H., & Broholm, M. M. (2017). Integrity of clay till aquitards to DNAPL migration: Assessment using current and emerging characterization tools. *Ground Water Monitoring & Remediation*, 37(3), 45-61. <https://doi.org/10.1111/gwmr.12217>

---

### **General rights**

Copyright and moral rights for the publications made accessible in the public portal are retained by the authors and/or other copyright owners and it is a condition of accessing publications that users recognise and abide by the legal requirements associated with these rights.

- Users may download and print one copy of any publication from the public portal for the purpose of private study or research.
- You may not further distribute the material or use it for any profit-making activity or commercial gain
- You may freely distribute the URL identifying the publication in the public portal

If you believe that this document breaches copyright please contact us providing details, and we will remove access to the work immediately and investigate your claim.

1 Integrity of clay till aquitards to DNAPL migration: Assessment using current and  
2 emerging characterization tools

3 Annika S. Fjordbøge<sup>a\*</sup>, Gry S. Janniche<sup>a,d</sup>, Torben H. Jørgensen<sup>b</sup>, Bernt Groesen<sup>b</sup>, Gary Wealthall<sup>c</sup>,  
4 Anders G. Christensen<sup>d</sup>, Henriette Kern-Jespersen<sup>e</sup>, Mette M. Broholm<sup>a</sup>

5 *<sup>a</sup>Department of Environmental Engineering, Technical University of Denmark, Bygningstorvet,  
6 Building 115, 2800 Kgs. Lyngby, Denmark; <sup>b</sup>COWI, Parallelsvej 2, 2800 Kgs. Lyngby, Denmark;*

7 *<sup>c</sup>Geosyntec Consultants, 130 Stone Road West, Guelph, Ontario N1G3Z2, Canada; <sup>d</sup>NIRAS,  
8 Sortemosevej 19, 3450 Allerød, Denmark; <sup>e</sup>Capital Region of Denmark, Kongens Vænge 2, 3400  
9 Hillerød, Denmark*

10 *\*Corresponding author. Tel.: +45 45 25 16 21; fax: +45 45 93 28 50; e-mail address:  
11 asfj@env.dtu.dk*

12

13 **Abstract**

14 Field investigations were carried out to determine the occurrence of tetrachloroethene (PCE)  
15 dense non-aqueous phase liquid (DNAPL), the source zone architecture and the aquitard integrity at  
16 a 30-50 year old DNAPL release site. The DNAPL source zone is located in the clay till unit  
17 overlying a limestone aquifer. The DNAPL source zone architecture was investigated through a  
18 multiple-lines-of-evidence approach using various characterization tools; the most favorable  
19 combination of tools for the DNAPL characterization was geophysical investigations, Membrane  
20 Interface Probe (MIP), core subsampling with quantification of chlorinated solvents, hydrophobic  
21 dye test with Sudan IV and Flexible Liner Underground Technologies (FLUTE) NAPL liners with  
22 activated carbon felt (FACT). While the occurrence of DNAPL was best determined by  
23 quantification of chlorinated solvents in soil samples supported by the hydrophobic dye tests (Sudan  
24 IV and NAPL FLUTE), the conceptual understanding of source zone architecture was greatly  
25 assisted by the indirect continuous characterization tools. Although mobile or high residual DNAPL  
26 ( $S_t > 1\%$ ) only occurred in 11% of the source zone samples (intact cores), they comprised 86% of

the total PCE mass. The data set, and associated data analysis, supported vertical migration of DNAPL through fractures in the upper part of the clay till, horizontal migration along high permeability features around the redox boundary in the clay till, and to some extent vertical migration through the fractures in the reduced part of the clay till aquitard to the underlying limestone aquifer. The aquitard integrity to DNAPL migration was found to be compromised at a thickness of reduced clay till of less than 2 m.

## **Introduction**

Dense non-aqueous phase liquids (DNAPLs) such as chlorinated solvents have been widely used and are common groundwater contaminants (Doherty, 2000; Mackay and Cherry, 1989). DNAPL release sites can have significant impacts on groundwater quality as the solubility of the chlorinated solvents may be several orders of magnitude above their regulatory limits. At DNAPL release sites where an aquifer is overlain by a clay aquitard, the groundwater quality in the aquifer will depend on the integrity of the clay aquitard as a barrier to the downwards migration of DNAPL. The low permeability clay aquitard will be associated with a high capillary resistance to DNAPL, which typically results in DNAPL pooling on top of the aquitard (Mercer & Cohen, 1990). Modelling of dual-porosity media has shown that further spreading of the contaminants may occur by transport of DNAPL in fractures, which are common in many aquitard systems, and in any coarser grained interbeds, and by the interrelated uptake of dissolved contaminants by matrix diffusion (e.g. Esposito & Thomson, 1999; Kueper & McWhorter, 1991; Parker et al. 1994, 1997; Reynolds & Kueper, 2001, 2004; Slough et al., 1999; VanderKwaak & Sudicky, 1996; Yang et al., 2012). Laboratory studies with both glaciolacustrine clay (O'Hara et al., 2000) and clay till (Jørgensen et al., 1998a) have shown that the fractures may act as rapid conduits for DNAPL migration in a manner that is difficult to predict. The integrity of the aquitard may therefore be compromised by extensive fracture systems. Observations of vertical fractures in Danish clay till show that fractures are common in the oxidized zone of the aquitard and that the likelihood of fracture development

53 throughout the entire clay till aquitard increases with decreasing thickness of the aquitard.  
54 Furthermore, the thickness of a less fractured reduced zone and the drainage conditions below the  
55 aquitard impact the extent of fractures (Klint et al., 2013). DNAPL migration in these fracture  
56 systems will be affected by the matrix diffusion. The dual-porosity media can provide a  
57 considerable retention capacity as the mass storage capacity of the matrix is generally much higher  
58 than the storage capacity of the fractures (Parker et al., 1997). Hence, a significant volume of  
59 DNAPL can be removed from the fractures through dissolution and subsequent diffusion to the  
60 aquitard matrix, which may prevent migration of DNAPL through the fractured aquitard. The  
61 specific entrapment and dissolution of DNAPLs will be very sensitive to heterogeneities in the  
62 media (Poulsen and Kueper, 1992) including variations in the fracture aperture or even small-scale  
63 variations in the individual fractures (Esposito & Thomson, 1999; Yang et al., 2012). Consequently,  
64 thorough characterization of DNAPL source zone architecture is essential in relation to  
65 management, risk assessment and remediation of sites with dual-porosity media.

66 The nature of the dual-porosity media, however, makes it difficult to locate the DNAPL and  
67 determine the source zone DNAPL architecture. Parker et al. (2004) have made detailed field  
68 investigations of the matrix diffusion of trichloroethene (TCE) into a glaciolacustrine clayey silt  
69 aquitard with DNAPL pooled on top of the formation. Further studies can be aided by current and  
70 emerging characterization tools for direct and indirect DNAPL detection such as: intact core  
71 subsampling with depth-discrete VOC quantification (e.g. Griffin & Watson, 2002; Parker et al.,  
72 2003; Rivett et al., 2014); hydrophobic dye test for direct visual confirmation of DNAPL through  
73 dye partitioning into the DNAPL e.g. Sudan IV (Cohen et al., 1992; Griffin & Watson, 2002; Parker  
74 et al., 2003; Rivett et al., 2014); FLUTE liners e.g. impregnated with a hydrophobic dye for visual  
75 confirmation of DNAPL upon contact with the liner membrane (Broholm et al., 2016; Griffin &  
76 Watson, 2002); Membrane Interface Probe (MIP) for continuous depth-discrete data obtained by  
77 volatilization of contaminants, diffusion through the semi-permeable membrane and vapor detection  
78 by e.g. Flame Ionization Detector (FID) (Adamson et al., 2014; Griffin & Watson, 2002; Rivett et

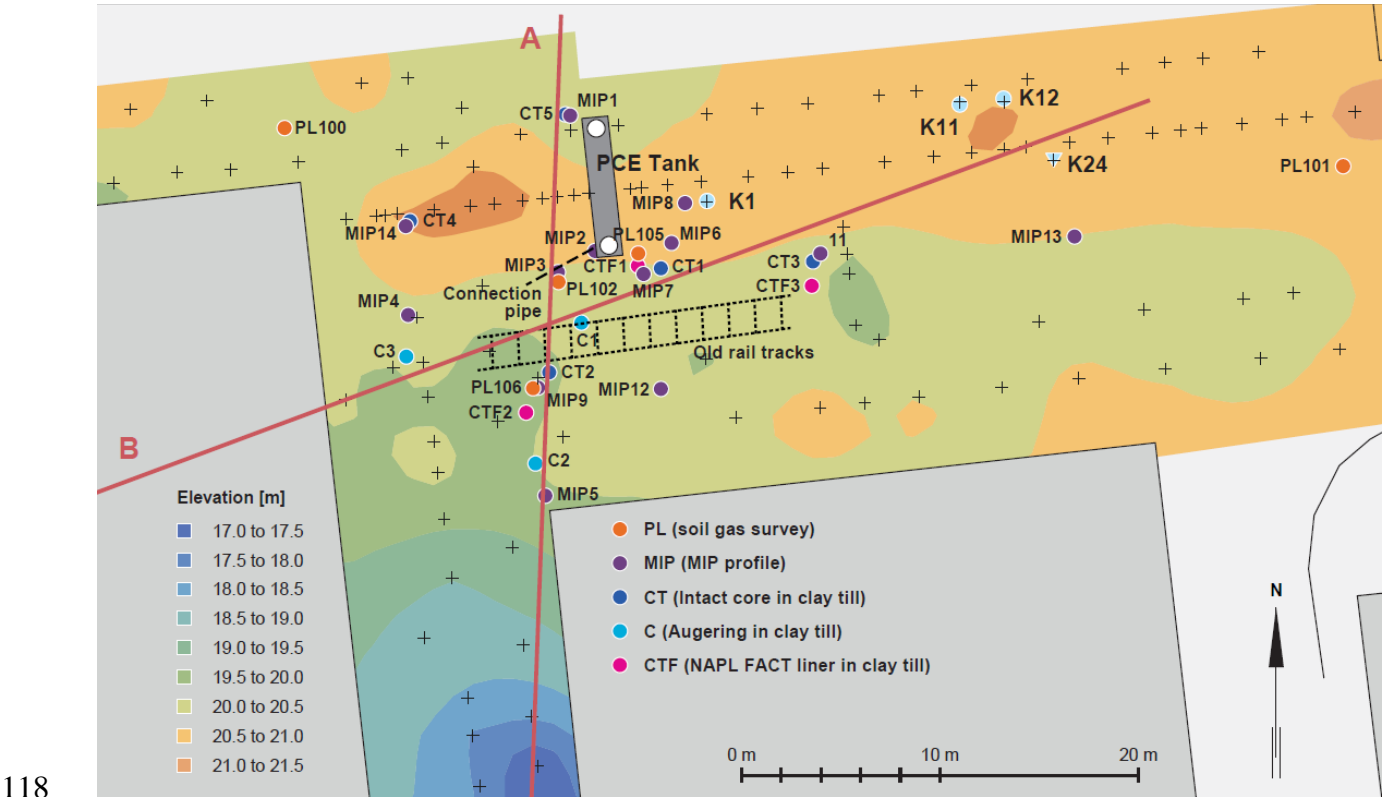
79 al., 2014); organic vapor analysis (OVA) screening of soil samples (headspace) or along intact cores  
80 with vapor detection by e.g. FID (Griffin & Watson, 2002); partitioning tracers (aqueous or  
81 gaseous) with an affinity to be detained in the DNAPL e.g. in the form of partitioning interwell  
82 tracer tests (PITT) (Hartog et al., 2010; Mariner et al., 1999) or soil gas surveys of natural occurring  
83 partitioning tracers such as radon,  $^{222}\text{Rn}$  (Höhener & Surbeck, 2004; Schubert et al., 2007; Semprini  
84 et al., 2000); Laser-Induced Fluorescence (LIF) with continuous depth-discrete detection of  
85 emissions from DNAPL with inherent fluorescent properties e.g. aromatic compounds (D'Affonseca  
86 et al., 2008; Kram et al., 2001) or the modified Dye-Enhanced LIF (Dye-LIF) with injection of a  
87 hydrophobic dye and subsequent detection of fluorescent changes in the presence of DNAPL e.g.  
88 chlorinated solvents (Germain et al., 2014); and the Waterloo profiler with depth-discrete low-purge  
89 collection of groundwater samples (direct push) (Parker et al., 2003; Pitkin et al., 1999). Some of  
90 these characterization tools have previously been combined in a multiple-lines-of-evidence  
91 approach and compared for DNAPL characterization at sandy industrial sites (Griffin & Watson,  
92 2002; Parker et al., 2003; Rivett et al., 2014). The use of these characterization tools at sites with  
93 strongly heterogeneous dual-porosity media is, so far, limited. When assessing the clay till aquitard  
94 integrity by a multiple-lines-of-evidence approach with the currently available characterization  
95 tools, near-continuous characterization tools are preferable as a high discretization is crucial in  
96 DNAPL characterization. The above characterization tools can also be supplemented with newer  
97 tools e.g. down-hole FLUTE liners with activated carbon felt (FACT).

98 The purpose of the investigations was to obtain a better conceptual understanding of the DNAPL  
99 source zone architecture (incl. chemical mass distribution) in fractured clay till aquitards, thereby  
100 improving the assessment of the integrity of the clay till aquitards in terms of aquifer protection and  
101 design of remedial actions at DNAPL release sites. The DNAPL source zone architecture was  
102 investigated by a combination of current and emerging site investigation methods for direct and  
103 indirect documentation of DNAPL, including most of the technologies mentioned above and the  
104 novel FLUTE Activated Carbon Technology. The characterization tools have mostly been applied to

105 aquifers and detailed studies on DNAPL migration in highly heterogeneous fractured clay tills  
106 aquitards are lacking.

107  
108 **Site description**

109 The field site is a former distribution facility for tetrachloroethene (PCE) and TCE located at  
110 Naverland near Copenhagen, Denmark (Fig. 1). The facility was operational for 18 years (1965-  
111 1983) where an estimated 5000 tons of PCE (subsurface tank, 1.0-2.5 m below ground surface  
112 (bgs)) and 1700 tons of TCE (barrels) were handled. The distribution activities resulted in PCE and  
113 TCE DNAPL impacts to the fill and the fractured clay till (vadose zone) from surface spillage of the  
114 chlorinated solvents and/or subsurface leakage of PCE from the tank and/or the connection pipe to  
115 the southwestern end of the tank. The groundwater table is located approximately 6.5 m bgs, and  
116 the groundwater concentrations also indicate that the underlying fractured limestone aquifer (around  
117 7-8 m bgs) may be impacted by DNAPL.



118  
119 **Fig. 1.** Overview map of the site with structures (buildings, the previous PCE storage tank with connection pipe, and  
120 part of the old rail tracks, north of which the solvents were unloaded), the clay till surface elevation (m above sea level),  
121 the 13 MIP profiles (MIP1-9, MIP11-14), the five intact clay till cores (CT1-5), the three auger drillings (C1-3), the

122 three FACT NAPL FLUTe installations (CTF1-3), and the five soil gas surveys (PL100-102, PL105-106). The red lines  
123 indicate part of the geological cross-sections (A and B) in Fig. 2.

124

125 **Materials and methods**

126 **Investigative approach**

127 Characterization of DNAPL architecture is challenging, and to improve the robustness of the  
128 conceptual model, a multiple-lines-of-evidence approach was utilized to obtain data for the  
129 conceptual model. The more consistent the different lines of evidence are with a DNAPL  
130 architecture scenario, the more plausible the given scenario. The lines of evidence approach  
131 combined site history (locations with DNAPL handling and storage), geological characterization  
132 (surface geophysics; redox boundary; fracture orientation, inclination, spacing and aperture; and  
133 saturation conditions) and a number of direct and indirect characterization tools for detection of  
134 DNAPL (Table 1) with different spatial data resolution.

135

136 **Table 1.** Selected characterization methods for direct/indirect and continuous/point determination of DNAPL.

	Direct methods	Indirect method
Continuous	Flexible liners (NAPL FLUTe)	Membrane Interface Probe (Electron Capture
	Hydrophobic dye tests (Indigo Blue spray)	Detector (ECD), FID)
		Concentrations on activated carbon (FACT FLUTe)
Point	Hydrophobic dye tests (Sudan IV)	Partitioning tracer (natural radon)
	Direct observations of DNAPL (water or soil)	Organic vapor analysis (OVA) by Photo Ionization
		Detector (PID) (soil samples)
		Calculations based on water, soil and/or pore air concentrations

137

138 Based on the site history, initial geological characterization was done in a 110x70 m area (surface  
139 geophysics) and along two cross-sections (50-75 m) to assess locations of possible DNAPL pooling  
140 on top of the clay till and preferential flow paths. MIP and soil gas surveys were used to delineate  
141 the most contaminated part of the DNAPL source area, the locations of these investigations were  
142 based on the site history and the geological characterization. The investigations in this area were  
143 supplemented with augering and intact coring with discrete subsampling (concentrations in clay till,



144 OVA, hydrophobic dye test) along with installation of FLUTe liners (NAPL, FACT) for method  
145 comparison. Since the characterization methods utilize adjacent boreholes ( $1\pm0.5$  m spacing), the  
146 results will be subject to natural variations in the DNAPL distribution, which is controlled by small-  
147 scale features. An overview of the different sampling locations is given in Fig. 1.

## 148 **Geological characterization**

149 The transition between different geological layers is based on: surface geophysics, i.e. ground  
150 penetrating radar (GPR) with a combination of 100 MHz and 250 MHz antennas and seismic  
151 reflection and refraction (SRR) using a Geometrics Geode Ultra-Light Exploration Seismograph;  
152 observations from augering and intact coring; electrical conductivity (EC) logging during the MIP  
153 profiling; and geophysical borehole logging (mainly gamma) of six existing wells. The surface  
154 geophysics were used to determine the transition between fill, clay till and limestone, while the  
155 observations from coring and logging were also used to assess the transition between the different  
156 clay till units. Furthermore, the coring and augering was used to determine the location of the redox  
157 zone in the clay till based on a color shift from oxidized yellowish brown to reduced (olive) gray.

158 The geological characterization was not sufficient for a thorough investigation of fractures;  
159 assumptions regarding fractures are, therefore, primarily based on the *a priori* knowledge of the  
160 ground moraine deposits typical in the Copenhagen area gathered through excavations at similar  
161 sites within the area (Christiansen et al., 2008; Jørgensen et al., 2003; Klint, 2001). Observations  
162 made during clay till core characterization are generally consistent with the *a priori* knowledge.  
163 Textural properties of clay till material at a nearby site (15-20 km) are given by Jørgensen et al.  
164 (1998b, 2002).

## 165 **Membrane Interface Probe (MIP) profiling**

166 A MIP-6520 heated probe with removable membrane and dipole electrical conductivity array was  
167 mounted on a 5400 Geoprobe (direct push drill rig) with a GH41 hydraulic hammer for probe rod  
168 advancement. The probe was heated to 120°C and the diffused gasses were collected by nitrogen  
169 carrier gas (40 mL/min) in a PTFE trunk line. The use of a halogen specific detector (ECD) was

170 combined with a detector for a broader range of organic compounds (FID). Near-continuous data  
171 were collected with a speed of 0.4-0.6 m/min; the data collection was only interrupted by  
172 subsampling of the carrier gas for analysis on a calibrated GC-MS (HP 6890). The sensitivity and  
173 carry-over was monitored by ongoing response tests (cf. SI for more details). The probe was also  
174 equipped with a sensor for continuous EC logging, where clay-rich units are represented by higher  
175 EC readings.

#### 176 **Soil gas survey of natural occurring partitioning tracer ( $\text{Rn}^{222}$ )**

177 The pore air was collected at 2-3 depths using a GeoProbe to place the probes. Back pressure, the  
178 PID value,  $\text{CO}_2$ ,  $\text{CH}_4$  and  $\text{O}_2$  were monitored until the soil gas probe was purged (stabilization) (cf.  
179 SI for more details). The pore air was analyzed for chlorinated solvents (GC, HP 6890) and  $\text{Rn}^{222}$   
180 (scintillation cells, duplicates). Due to analytical issues associated with the chlorinated solvents, the  
181 data are only used qualitative to indicate likely DNAPL presence in areas where DNAPL has been  
182 confirmed by other methods.

#### 183 **Sampling of the clay till units**

##### 184 *Intact core collection and subsampling*

185 The intact coring was done by the GeoProbe Dual-Tube system (1.5" ID) at five locations. The  
186 cores were retrieved in PVC liners (38 mm wide; 1.2 m long), which were sealed with PVC  
187 stoppers and adhesive tape. The samples were stored vertically (same orientation as in the  
188 subsurface) at 10°C until they were subsampled (within 4 days). The intact cores were initially split  
189 in half lengthwise and subsampled in a ventilation hood. One half was utilized for hydrophobic dye  
190 test (Indigo Blue), while the other half was subsampled for chlorinated solvents analysis (pentane  
191 extraction; 258 samples in total), hydrophobic dye test (Sudan IV; 56 samples in total) and OVA  
192 readings (PID; 64 samples in total). Subsampling of the cores was done by small core drills (0.5-1  
193 cm ID) with a plunger. Subsamples were generally collected at high resolution around any observed  
194 larger fractures/lenses and/or at a set interval depending on the type of test. After the cores had been

195 subsampled for DNAPL characterization, a more meticulous geological assessment was performed  
196 for better insight into the small-scale geologic features of the source zone (cf. SI for more details).

#### 197 *Augering*

198 Clay till samples were collected with a discretization of 0.5 m at depths between 1.0-8.0 m bgs at  
199 three additional locations (C1-C3) using augering equipment (the geology was documented during  
200 the field work). The clay till was sampled for chlorinated solvents analysis (pentane extraction),  
201 OVA screening (PID) and occasionally hydrophobic dye tests (Sudan IV). Additionally, certain clay  
202 till characteristics (porosity, bulk density, dry matter and water saturation) were determined based  
203 on six subsamples collected between 1.5-6.0 m bgs at C1.

#### 204 *Quantitative analysis*

205 The clay till subsamples were extracted (using pentane) for analysis of chlorinated solvents. A  
206 known amount (by weight) of water (10 mL), clay till (5 g) and pentane (5 mL) were added to the  
207 extraction vial (40 mL VOA vial). The vial was vigorously shaken (vortex mixer) and placed in a  
208 rotation box at 10°C until the following day when the pentane was extracted and analyzed by GC-  
209 MS.

#### 210 *Organic vapor analysis*

211 The organic vapor was analyzed using a Microtip 10.6 eV Krypton PID lamp calibrated with  
212 isobutylene gas. The cores were screened by running a handheld PID along the surface. Samples  
213 were collected and transferred to Rilsan® diffusion-proof bags, which were closed with headspace  
214 and stored at 4°C until the following day. Before the PID analysis of the headspace, the samples  
215 were acclimatized to room temperature (>4 hours).

#### 216 *Hydrophobic dye test*

217 Two types of hydrophobic dye test kits from Cheiron Resources Ltd. were used i.e.  
218 OilScreenSoil® (Sudan IV) containing the hydrophobic red dye Sudan IV and a water soluble  
219 fluorescent green dye and OilScreenDNAPL-LENS Spray® containing the hydrophobic blue dye  
220 Indigo Blue (cf. SI for more details).

221 **Flexible Liner Underground Technology (FLUTe)**

222 The FLUTe is a tubular urethane coated nylon liner (Cherry et al., 2007). The liner was installed  
223 with GeoProbe (direct push) in three boreholes (CTF1-CTF3) as close as possible (approximately 1  
224 m) to the intact cores collected at CT1-CT3. The inside-out flexible liner was attached to the casing  
225 (5.7 cm or 2.25”) and pushed through the subsurface with the GeoProbe. The liner had a  
226 polyethylene pipe for air and/or water addition tethered inside the interior bottom of the liner. As  
227 the casing was withdrawn the liner was filled with air (0.7 bar) to push the liner against the borehole  
228 wall. Once the casing was removed the liner was filled with water (4.1 bar) to maintain the interior  
229 pressure against the borehole wall. Retraction was done by pulling the tether and inverting the liner.  
230 The liner was exposed to the borehole wall for 24 hours before retraction.

231 The liner was equipped with a NAPL FLUTe dye impregnated membrane. During the inside-out  
232 exposure of the liner in the borehole (24 hours) the membrane was in contact with the clay till  
233 formation. Any direct contact with NAPL in the formation should activate the dye and thereby form  
234 visible stains on the membrane. The liner was also equipped with a longitudinal strip of highly  
235 porous activated carbon felt, referred to as FACT. During exposure in the borehole, the FACT,  
236 contained within a diffusion barrier, was pushed against the clay till formation, which should result  
237 in sorption of the contaminant through contact with DNAPL, pore water and/or pore air. After  
238 retraction of the liner, the NAPL membrane was inspected on-site by cutting the inverted liner open;  
239 the locations of NAPL stains were documented. The FACT was cut in half lengthwise and  
240 subsampled in discrete subsections of 2-10 cm. The FACT subsamples were extracted (using  
241 pentane) for analysis of chlorinated solvents. A known amount (by weight) of water (10 mL),  
242 pentane (3 mL) and (by dimensions) FACT (0.06-0.32 g) were added to the extraction vials (20 mL  
243 VOA vials). At the end of the day, the vials were placed in a rotation box at 10°C for 84 hours  
244 before the pentane was extracted and analyzed on GC-MS.

245 **GC-MS analysis**

246 The pentane extracts from the clay till sampling and the FACT were analyzed by GC-MS using an  
 247 Agilent 7980 gas chromatograph system equipped with an Agilent 5975C electron impact (70 eV)  
 248 triple-axis mass-selective detector with a 30 m x 0.25 mm I.D x 1.40 µm film thickness ZB-624  
 249 capillary column (Phenomenex). Chloroform was used as the internal standard and detection and  
 250 quantification limits were determined as described by Winslow et al. (2006) (cf. SI for details).

## 251 **Data analysis**

252 The DNAPL threshold concentration,  $C_T$ , of the chlorinated solvents in the clay till above which  
 253 the presence of DNAPL would be suspected was calculated based on partitioning theory (Feenstra  
 254 et al., 1991):

$$255 \quad C_T = S \cdot x \frac{K_d \rho_b + n_w + n_a K_H}{\rho_b}, \quad (1)$$

256 where  $S$  is the solubility of the compound,  $x$  is the molar fraction of the compound,  $K_d$  is the  
 257 partitioning coefficient between pore water and soil,  $\rho_b$  is the bulk density,  $n_w$  is the water-filled  
 258 porosity,  $n_a$  is the air-filled porosity and  $K_H$  is the dimensionless Henry's law constant.

259 The DNAPL saturation can be given as the saturation of the total porosity,  $S_t$ :

$$260 \quad S_t = (C_{Total} - C_T) \frac{\rho_b}{\rho_{DNAPL} n_t}, \quad (2)$$

261 where  $C_{Total}$  is the total amount of the chlorinated compound in the soil,  $n_t$  is the total porosity and  
 262  $\rho_{DNAPL}$  is the density of the DNAPL.

263 When considering the DNAPL saturation in a dual-porosity media, it can be relevant to  
 264 distinguish between the total porosity and the fracture porosity. The fracture porosity,  $n_f$ , is given as  
 265 (McKay et al., 1993):

$$266 \quad n_f = 2 \frac{2b}{2B}, \quad (3)$$

267 where  $2b$  is fracture aperture and  $2B$  is fracture spacing.

268 Site specific values were obtained for the porosity ( $n_t$ ,  $n_w$ ,  $n_a$ ), bulk density,  $\rho_b$ , and dry matter  
 269 (samples from C1); the average values were  $n_t$  of 0.27 ( $\sigma = 0.01$ ),  $n_w$  of 0.24,  $n_a$  of 0.03,  $\rho_b$  of 1.96  
 270 kg/L ( $\sigma = 0.03$  kg/L) and dry matter of 91 % ( $\sigma = 2$  %). The  $K_d$  values used for clay till were

determined at two similar clay till sites within 10 km of the Naverland site, and the values were 1.37 L/kg [0.84-2.45 kg/L] and 0.85 L/kg [0.62-0.96 kg/L] for PCE and TCE, respectively (Lu et al., 2011). The solvent densities used were 1.63 kg/L and 1.46 kg/L and the water solubilities were 0.00024 kg/L and 0.0014 kg/L for PCE and TCE, respectively (Broholm & Feenstra, 1995), while the dimensionless Henry's law constants used were 0.75 and 0.40, respectively (Pankow & Cherry, 1996).

277

## 278 **Results and discussion**

### 279 **Site geology**

280 The geophysics and the drilling/coring at the site showed an overall geology with a vadose zone  
281 consisting of a fill layer (0-1 m bgs) and two fractured clay till units (1-7 m bgs), an upper more  
282 fractured unit (ML1) and a lower sandier unit (ML2) (Fig. 2). The redox boundary was located  
283 around 5.0 m bgs ( $\sigma = 0.8$  m) with a local depression in the area around CT2, C1 and C3. The EC  
284 logging confirms transitions around 2.8 m bgs (ML1 to ML2) and 4.5 m bgs (redox transition) (cf.  
285 SI, Fig. S1). The local fluctuations in the position of the redox boundary are likely linked to  
286 variations in the development of vertical fractures, whereby locally more developed fractures will  
287 result in a deeper lying redox boundary. According to Klint et al. (2013), Danish field observations  
288 show a medium to high likelihood of fractures throughout the clay till aquitard at sites where the  
289 thickness is less than 8-10 m (reduced clay till <3 m). This applies to the Naverland site, where the  
290 clay till layer is around 6 m thick (reduced layer of 1-3 m).

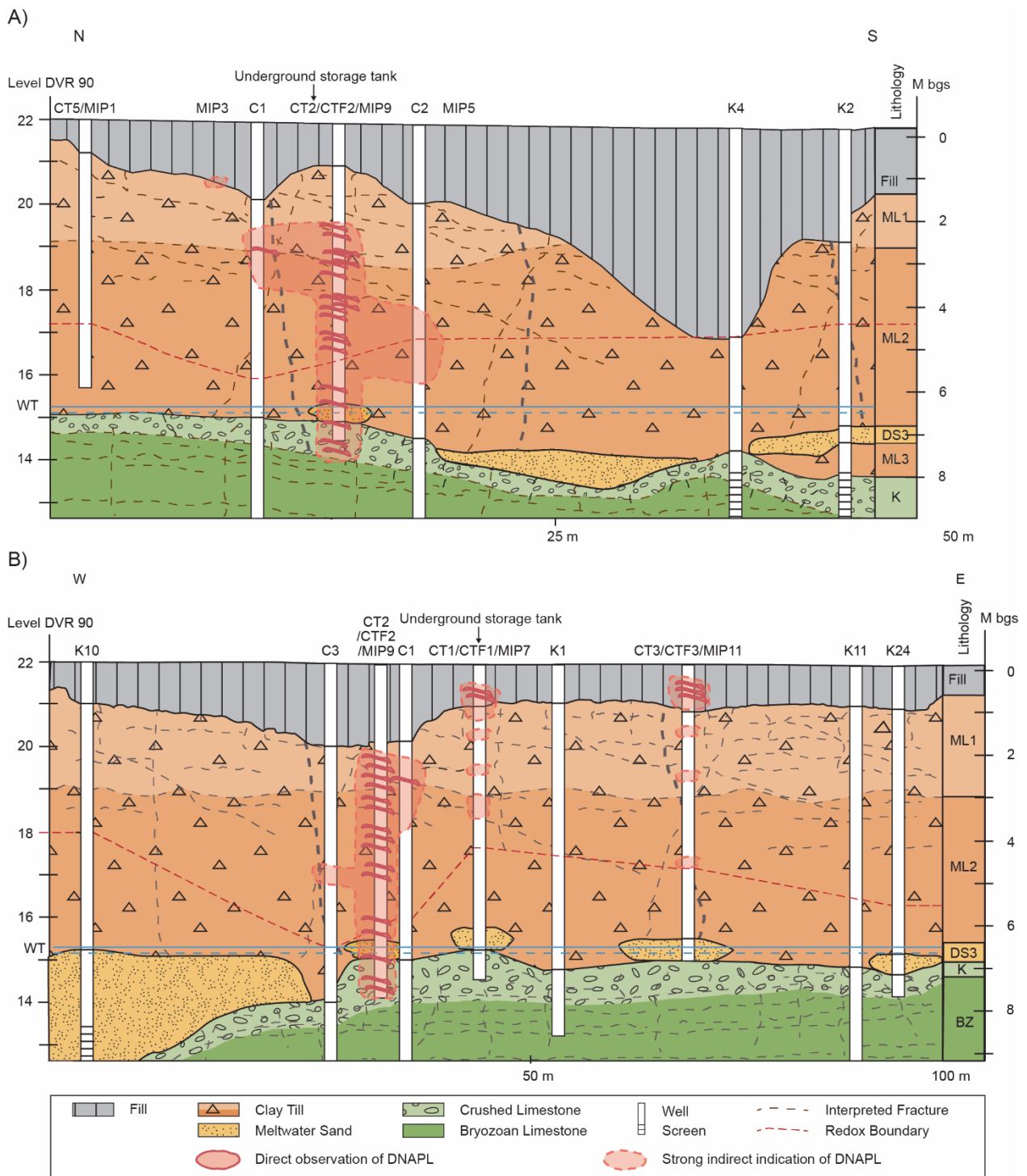


**Fig. 2.** Conceptual site geology (cf. cross-sections A and B on Fig. 1) with the approximate location of the redox boundary and direct observations and strong indirect indications of DNAPL. Fractures are interpreted fractures representing the higher frequency in the upper clay.

The inclination and orientation of the geological surfaces and fractures are of great importance for understanding the potential migration of DNAPL in the clay aquitard. The geophysics at the site showed that the surface of the clay till formation was generally dipping towards the S/SW (Fig. 1).

300 The glacial deposits in the area are associated with advances of Baltic ice from the southeast (Kjær  
301 et al., 2003). The fractures in the clay till generally originate as glacial-tectonic (sub-horizontal  
302 shear, conjugating sub-vertical shear and vertical extension) and contraction (freeze-thaw and  
303 desiccation) fractures. The vertical extension fractures are oriented in the direction of the ice  
304 movement (SE-NW), while the sub-vertical shear fractures are oriented perpendicularly to the ice  
305 movement (SW-NE). The shear fractures generally have an inclination dipping in the same  
306 direction as ice advancement (Klint, 2001), where the most developed fractures have an inclination  
307 dipping towards the SE, while a less developed fracture system has an inclination dipping towards  
308 the NW (ice recession and ice advancement, respectively).

309 The contraction fractures have a more irregular orientation and become less frequent with depth  
310 (Klint, 2001; McKay et al., 1993). The upper 3.5-5 m above the redox boundary are expected to be  
311 impacted by numerous contraction fractures. Observations showed an average fracture spacing of  
312 around 30 cm in the upper 3-4 m. Fracture spacing has been classified for 13 Danish clay sites  
313 (Jørgensen et al., 2003; Klint, 2001). The spacing above the redox boundary is generally 5-30 cm,  
314 while it gradually increases below the redox boundary with a spacing of 40-180 cm at 7 m bgs  
315 (Jørgensen et al., 2003). For Danish sites, clay till fracture apertures of 10-80  $\mu\text{m}$  have been  
316 reported (Jørgensen et al., 1998b, 2002), which is similar to values reported for other clay tills (e.g.  
317 McKay et al., 1993). An average fracture aperture of 50  $\mu\text{m}$  has been reported for clay till  
318 (Jørgensen et al., 2002; McKay et al., 1993).

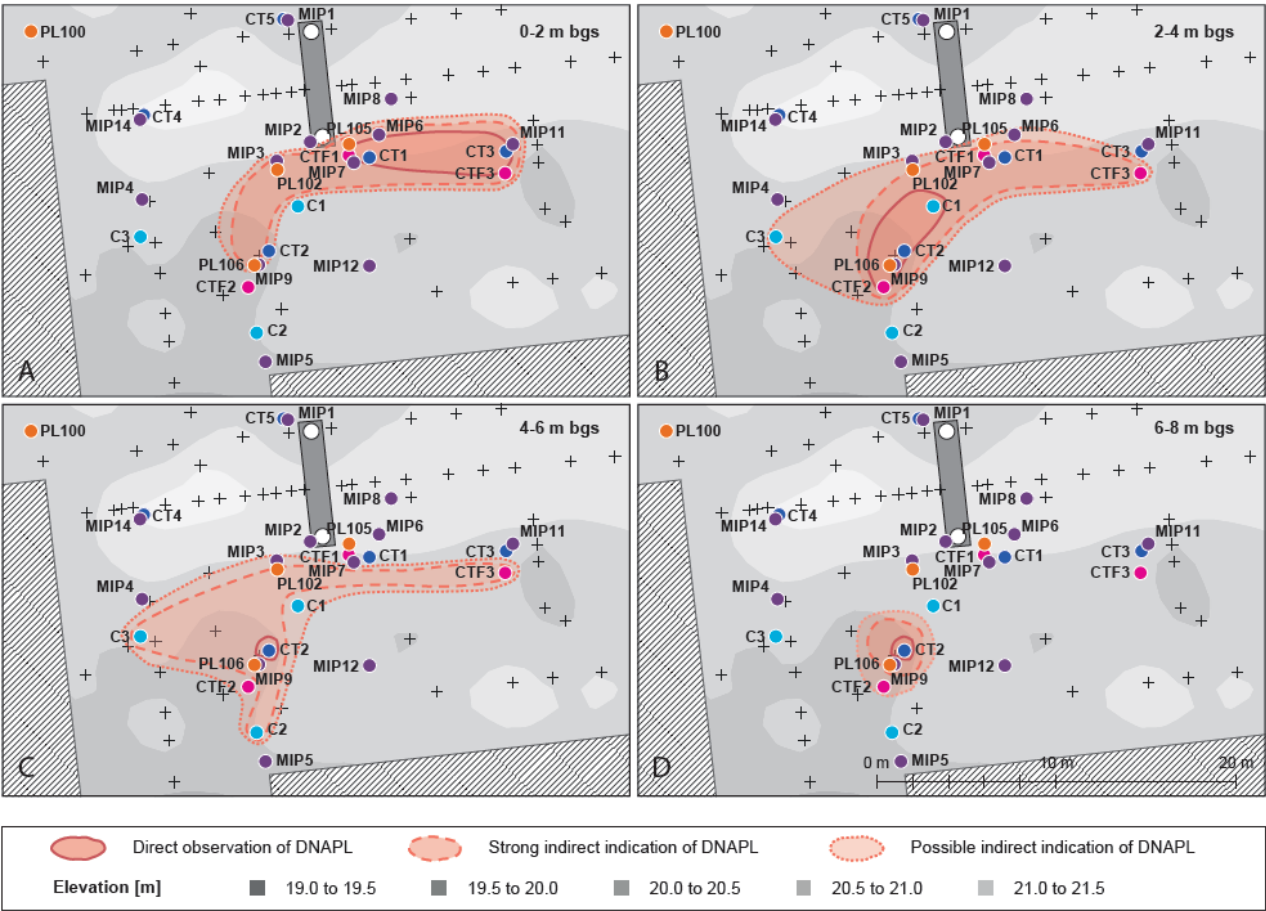
319 Above the groundwater table, the clay till matrix is generally considered to be saturated, while the  
320 fracture systems are unsaturated. The water saturation is lower in the upper part of the clay till (67  
321 % at 1.5 m bgs), and increases to 88 % ( $\sigma = 2.5$  %) at 3.0-5.0 m bgs. The groundwater flow will  
322 predominantly be vertical through the larger fractures. The clay till is underlain by a thick bryozoan  
323 limestone aquifer, where the transition zone between the clay and the limestone consists of  
324 approximately 1 m of sand, gravel and brecciated limestone. According to Klint et al. (2013), the  
325 occurrence of fractures in the clay aquitard is increased if the underlying aquifer offers well-drained



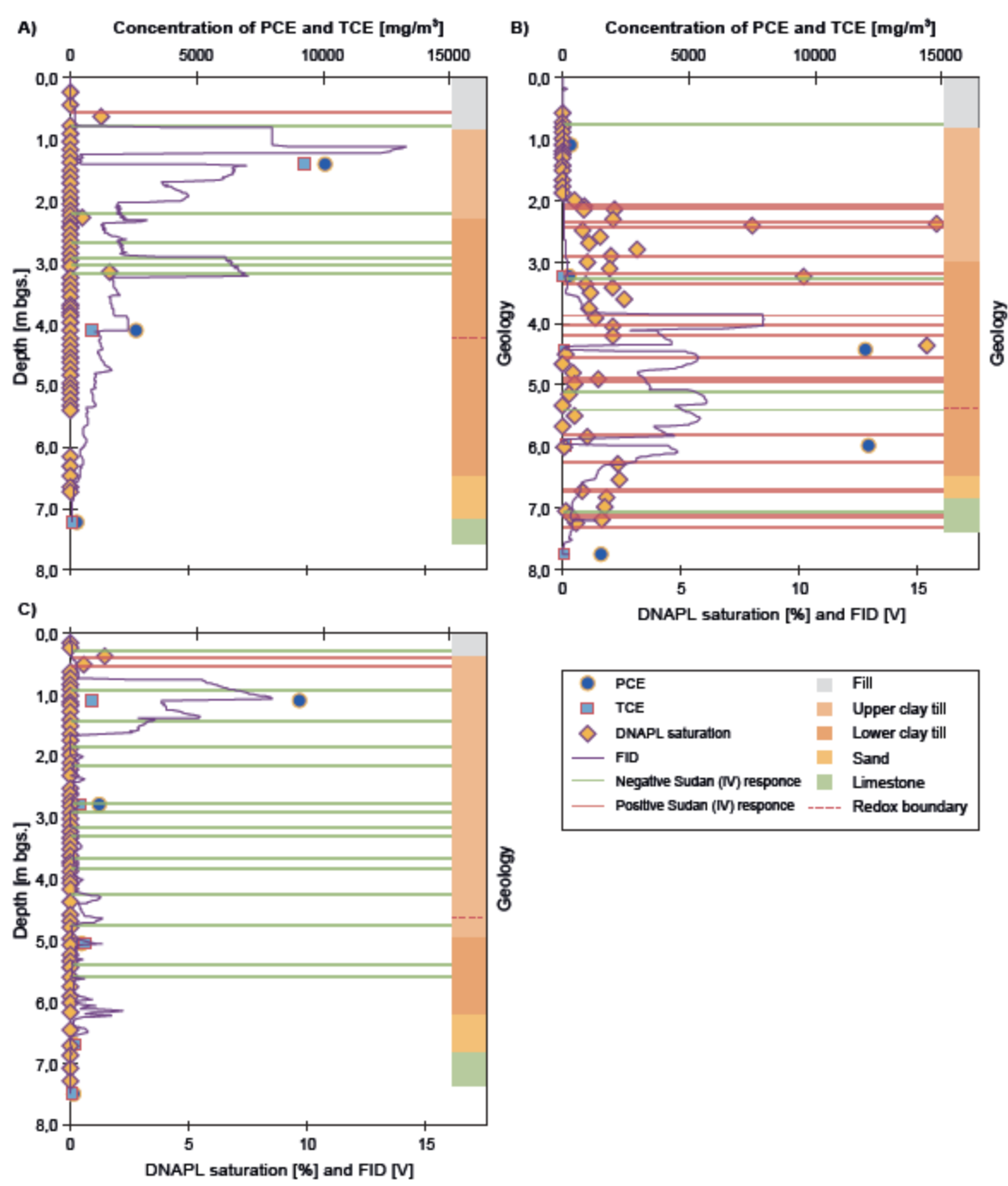
326 conditions as the subglacial drainage conditions are a key factor for the deformation mode (ductile  
 327 or brittle) of basal clay tills. The well-drained B-type basal till (brittle deformation) is more  
 328 heterogeneous with systematic fractures. A highly transmissive aquifer, like the one at the  
 329 Naverland site, will thereby increase the likelihood of fractures fully penetrating the clay till unit.  
 330 Based on the geology at the site, there is a relatively high risk that DNAPL could migrate though  
 331 (sub-)vertical fractures in the clay till aquitard to the underlying limestone aquifer.

332 **DNAPL migration**

333 While the characterization tools can be used to assist in the horizontal delineation of the DNAPL  
 334 source area (cf. Fig. 3), the main focus of the investigations was on the vertical migration of  
 335 DNAPL within the source area for the assessment of the integrity of the fractured clay till aquitard.  
 336 Most of the characterization tools were therefore focused on obtaining a vertical delineation of  
 337 DNAPL. A comparison of methods for three points is presented in Fig. 4 and Fig. 5, while two  
 338 additional locations are included in the SI (Fig. S2).

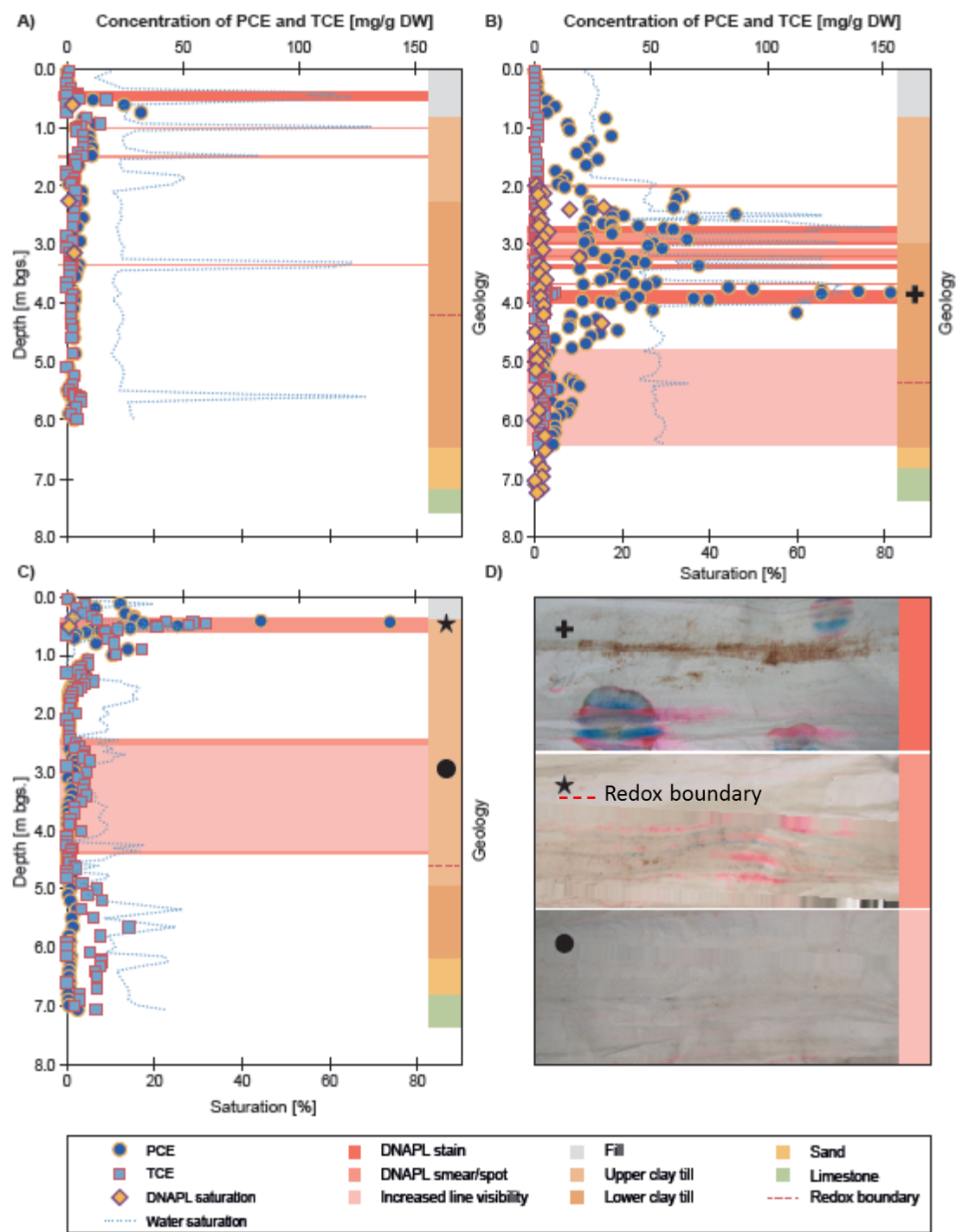


340 **Fig. 3.** Delineation of the horizontal DNAPL distribution in the source area in four depth intervals. The red lines  
 341 indicate: direct observation of DNAPL by dye colorization test i.e. Sudan IV or NAPL FLUTe; strong indirect  
 342 indication of DNAPL by contaminant concentration ( $S_T > 0\%$ ), NAPL FLUTe smearing/spotting, high MIP response  
 343 ( $FID \geq 5\text{ V}$ ), or high soil air concentrations ( $PID > 4000\text{ ppm}$ ); and possible indirect indication of DNAPL by NAPL  
 344 FLUTe transparency (increased transparency of line colors through the membrane), medium MIP response ( $2.5\text{ V} <$   
 345  $FID < 5\text{ V}$ ), or medium soil air concentrations ( $2000\text{ ppm} < PID < 4000\text{ ppm}$ ).  
 346



347

348 **Fig. 4.** Comparison of: DNAPL saturation (% of total porosity); PCE and TCE concentration (mg/m<sup>3</sup>) in the carrier  
 349 gas; MIP FID signal (V); and Sudan IV color response. a) CT1 + MIP7; b) CT2 + MIP9; and c) CT3 + MIP11.  
 350



351  
 352 **Fig. 5.** DNAPL saturation (% of total porosity, only  $S_t > 0$  % is included), water saturation (%) of the FACT material  
 353 (not formation), PCE and TCE FACT concentration (mg/g DW) and NAPL FLUTE response comparison. The three  
 354 pictures indicate the typical extent of staining (staining, smearing and transparency) on the FLUTE NAPL liner at the  
 355 given color shade. a) CT1 + CTF1; b) CT2 + CTF2; c) CT3 + CTF3.

356

357 *Clay till samples*

358 The intact core recovery was generally good with an average recovery of 86 % ( $\sigma = 20$  %). The  
359 average recovery was affected by a few unsuccessful core recoveries; while the majority of the  
360 cores had excellent recovery of more than 95 %. The discrete subsampling with quantification of  
361 chlorinated solvents was used as a reference for the other methods.

362 The main constituent of the DNAPL was PCE with an average TCE molar fraction of 0.031 ( $\sigma =$   
363 0.001). This is the case for the deeper laying DNAPL in the area southwest of the PCE tank (cf. Fig.  
364 3), which likely originates from PCE leakage with TCE as an impurity. Locally, TCE molar  
365 fractions were higher (up to 0.49) close to the surface, especially in the area southeast of the PCE  
366 tank, where the DNAPL likely originates from spillage of solvents handled at the surface.

367 Based on the average DNAPL composition, the calculated DNAPL threshold concentrations (eq.  
368 1) are 317 mg/kg for PCE [206-545 mg/kg] and 39 mg/kg for TCE [30-43 mg/kg]. The DNAPL  
369 threshold concentration is sensitive to sorption, the given concentration ranges indicate the possible  
370 variation in DNAPL threshold concentrations based on the variation found in  $K_d$  values for Danish  
371 clay till (Lu et al., 2011). The indicated variations in  $K_d$  values will have a limited effect on the  
372 calculated (eq. 2) DNAPL saturations ( $\pm 0.2$  %). The threshold concentrations are exceeded at three  
373 out of five intact core sampling locations (CT1-CT3) (Fig. 4).

374 The dye tests with Sudan IV for direct identification of DNAPL worked well for determination of  
375 PCE (or mixed PCE/TCE) DNAPL (Fig. 4). A color reaction was never observed in adjacent clay  
376 till samples containing PCE concentrations less than 250 mg/kg (below calculated DNAPL  
377 threshold), while concentrations of PCE in adjacent clay till samples above 1500 mg/kg (equal to  
378 0.5 % DNAPL saturation of the total porosity) consistently resulted in coloration (cf. Fig. S4, SI).  
379 For the clay till samples with PCE concentrations in the in-between interval (250-1500 mg/kg),  
380 variable results were observed. This could be a result of false negatives due to interpretation issues  
381 with weak coloration or DNAPL dissolution at lower DNAPL saturations ( $< 0.5$  % of the total

382 porosity) and/or the variability in DNAPL saturation at even short distances, whereby the reference  
383 concentration in the nearest clay till subsamples is not representative for the actual subsample used  
384 for the dye test.

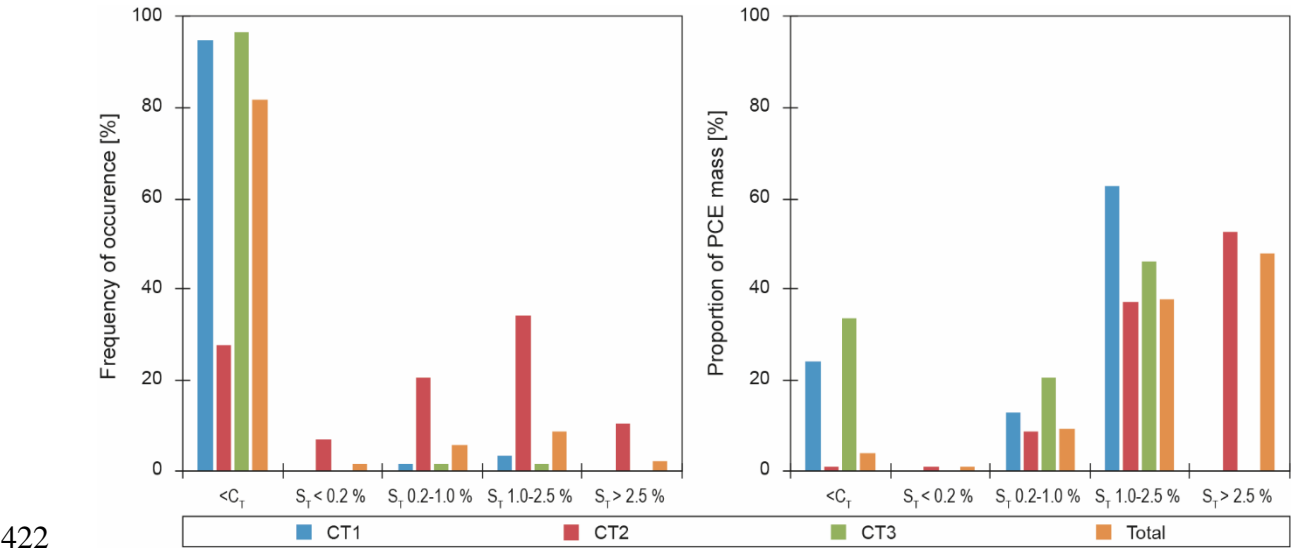
385 The blue-dye OilScreenDNAPL-LENS Spray® did not result in any visible coloration on the  
386 grey/brown clay till cores. This was also the case for cores where DNAPL had been confirmed at  
387 the opposite core half using the Sudan IV dye test. Hence, the spray was not a useful tool for  
388 DNAPL determination at this clay till site.

389 The final measurement on the samples from the intact cores and the augering was OVA by PID  
390 (cf. Fig. S3 in SI for maximum values). In previous studies with OVA by FID, readings exceeding  
391 1000 ppm (Cohen et al., 1992) or 3000 ppm (Griffin & Watson, 2002) have been used to infer areas  
392 associated with DNAPL (confirmed by other methods). When comparing the PID results of this  
393 study with the calculated DNAPL threshold concentrations in samples from approximately the same  
394 depth, the PCE concentrations were always above the threshold in the samples where  $PID > 4000$   
395 ppm. PID values  $> 4000$  ppm were also correlated with 90 % of the Sudan IV tests that were  
396 positive for DNAPL. The threshold was never exceeded when  $PID < 1000$  ppm and all Sudan IV  
397 tests were negative for DNAPL at  $PID < 1500$  ppm (cf. Fig. S5-6, SI). For PID values between  
398 1000-4000 ppm, indications of DNAPL varied; for  $PID < 3000$  ppm only two indications of  
399 DNAPL were found, while mixed indications were linked with PID of 3000-4000 ppm.

400 For two of the locations (CT1 and CT3), DNAPL was only directly observed (dye test) at the top  
401 of the upper clay till unit with indirect indications of DNAPL in the oxidized clay till. For the third  
402 location (CT2), DNAPL was directly observed (dye test) from 2 m bgs and throughout both clay till  
403 units. CT2 is located in the area with a depression in the redox boundary; hence the presence of  
404 DNAPL throughout the clay till units may be associated with locally more developed vertical  
405 fractures in that area (cf. Site geology section). The DNAPL threshold concentrations were also  
406 exceeded for the three less discretized augering locations C1-C3 (cf. Fig. 2), which are all located  
407 close to CT2 (3-8 m), with DNAPL saturations of up to 4 % (direct observation of DNAPL by

408 Sudan IV), 2 % and 0.5 %, respectively. This is consistent with a deeper occurrence of DNAPL in  
 409 the southwestern direction from the subsurface PCE tank (cf. Fig. 3). Hence, DNAPL spreading  
 410 may occur in sub-vertical shear fractures with a NE-SW orientation (cf. Site geology section).

411 The data on the DNAPL threshold concentrations are summarized (Fig. 6) with regard to the  
 412 frequency of occurrence and the mass distribution for each of the three intact coring locations with  
 413 DNAPL (CT1-3) and for the total area (all five intact coring locations). The grouping of data is  
 414 inspired by drainable core technique observations by Parker et al. (2003), where  $S_t < 10 \%$  is linked  
 415 with residual DNAPL (in a sandy aquifer) and on the grouping by Rivett et al. (2014) for a sandy  
 416 aquifer (no DNAPL if  $< C_T$ ; trace DNAPL if  $S_t < 1 \%$ ; moderate residual DNAPL if  $S_t = 1-10 \%$ ;  
 417 high residual DNAPL if  $S_t = 10-20 \%$ ; and pooled DNAPL if  $S_t > 20 \%$ ). The grouping has been  
 418 modified to better suit a fractured media. Also, a lower uncertainty is involved with the trace  
 419 DNAPL group. Hence the data is grouped in: no DNAPL ( $< C_T$ ), trace DNAPL ( $S_t < 0.2 \%$ ),  
 420 moderate residual DNAPL ( $S_t = 0.2-1 \%$ ), high residual DNAPL ( $S_t = 1-2.5 \%$ ) and mobile DNAPL  
 421 ( $S_t > 2.5 \%$ ).



422 **Fig. 6.** Frequency of occurrence and the PCE mass distribution for each of the three locations with DNAPL above the  
 423 threshold concentrations (CT1, CT2 and CT3) and for the total area (all five sampled locations). The data classification  
 424 is inspired by the one used by Rivett et al. (2014). The classification is: No DNAPL ( $< C_T$ ); trace DNAPL ( $S_t < 0.2 \%$ );  
 425 moderate residual DNAPL ( $S_t = 0.2-1 \%$ ); high residual DNAPL ( $S_t = 1-2.5 \%$ ); and mobile DNAPL ( $S_t > 2.5 \%$ ).  
 426

427

428 The trace DNAPL (<0.2 %) class is based on the uncertainty involved with the  $K_d$  values ( $\pm 0.2$   
429 %). The residual DNAPL classes (moderate at 0.2-1 % and high at 1-2.5 %) are based on repeated  
430 observations of DNAPL throughout CT2 in this saturation interval (Fig. 4), while large NAPL  
431 FLUTE stains are found less frequent (Fig. 5) and therefore linked to mobile DNAPL at a higher  
432 saturation (>2.5 %). The divide between the moderate residual DNAPL (0.2-1 %) and high residual  
433 DNAPL (1-2.5 %) class is somewhat more arbitrary. In CT2 it was found, that the FLUTE  
434 transparency (5-6 m bgs) generally occurs at DNAPL saturations below 1 %, therefore the division  
435 at 1 %.

436 The occurrence of mobile DNAPL at significantly lower DNAPL saturations than in a granular  
437 media (Parker et al., 2003; Rivett et al., 2014) is ascribed to the fractures where the main DNAPL  
438 migration occurs in the dual-porosity media. Considering a realistic range of fracture apertures (10-  
439 80  $\mu\text{m}$ ) and fracture spacing (10-100 cm) the fracture porosity will constitute <0.01-0.60 % of the  
440 total porosity (eq. 3). This would indicate that the fractures are potentially completely saturated at  
441 most of the locations with DNAPL. However, since the subsamples, that the calculated DNAPL  
442 saturations are based on, represent small volumes, which were often collected at observed fractures,  
443 the fracture constitutes a larger part of the total porosity than it would on the overall field scale with  
444 larger fracture spacing; e.g. a 50  $\mu\text{m}$  fracture would constitute 1.9 % of the total porosity in a 1 cm  
445 wide sample ( $n = 0.27$ ) or 0.4-3.0 % for the 10-80  $\mu\text{m}$  fracture range. This makes it reasonable to  
446 assume that mobile DNAPL could occur already at a DNAPL saturation of 2.5 % of the total  
447 porosity in the fractured media.

#### 448 *MIP*

449 Due to high signal response for halogenated compounds, the ECD was unfortunately prone to  
450 overload (>845 V) and subsequent carry-over/drag-down at chlorinated solvent concentrations in  
451 the adjacent clay till samples far below (<10 %) the calculated DNAPL threshold concentration.  
452 Thereby the ECD was too sensitive to be used at the DNAPL source zone. This is consistent with

findings by Adamson et al. (2014), where overload and carry-over/drag-down for the ECD is observed at their “high concentration” area (<40 mg/kg CVOC).

Adamson et al. (2014) also used the less sensitive PID and FID for contaminant characterization in the saturated low permeable zones. However, the FID data were not evaluated beyond initial screening as the response was negligible. In the case of DNAPL, the low FID response to the chlorinated solvents can be a desirable trait making it more suitable as a characterization tool. In our case the FID response was significant, while not exceeding the measuring range (<15 V). The FID signal is not halogen specific and the relative response of PCE, TCE and DCE can be expected to be more or less the same with only very small differences due to the slight inhibitory effect on the response from the chlorine atoms (McDermott, 2004); however, the GC-MS subsamples (chlorinated ethenes, chlorinated ethanes and BTEX) confirmed that the response was mainly due to PCE and TCE.

For the locations without DNAPL (CT4-5) a reasonable linear correlation ( $r^2 = 0.750$ ) was found between the sum of chlorinated solvent concentrations in the clay till samples and the average FID response in the adjacent sampling depths (cf. Fig. S7a, SI). These locations had a maximum concentration of chlorinated solvents (PCE and TCE) of 130 mg/kg and FID response of 1.2 V. For the locations with DNAPL (CT1-3), no linear correlation could be found ( $r^2 < 0.01$ ) (cf. Fig. S7b, SI). This is not surprising as the most significant FID response peaks and the maximum chlorinated solvent concentrations in the adjacent cores are not exactly aligned, indicating a significant spatial variation even within relatively small distances (<1 m). Still, the overall trends from CT1-CT5 were captured reasonable well by the nearby MIP7, MIP9, MIP11, MIP14 and MIP1 (cf. Fig. 4 and Fig. S2 in SI).

While no direct correlation between FID responses and DNAPL saturation could be made, the MIP profiles (6, 7, 9, 11) representing the DNAPL source zone (DNAPL confirmed by dye tests in nearby cores) gave maximum FID responses between 4.8 V and 14.2 V, whereby FID responses above 5 V give a strong indication that DNAPL is present at the location. The MIP profiles outside



479 the DNAPL source area (no DNAPL confirmation or indication in nearby cores) had maximum FID  
480 responses of 2.1 V. It is therefore unlikely to find DNAPL if the FID response is consistently below  
481 2.5 V given response tests of the same magnitude (15-75 mV response was observed for FID at 5  
482 mg/L PCE solution).

483 Although no direct correlation was found, the MIP profiling showed significant variations in the  
484 FID response and was useful as a screening tool for both vertical and horizontal delineation of the  
485 DNAPL area in the low permeable clay till in the vadose zone. The findings were consistent with  
486 the historical knowledge on the site. Shallow contamination was found in the eastern part of the  
487 area (MIP11, 13) with surface handling of solvents and deeper contamination starting around the  
488 redox boundary in the western part of the area (MIP2, 4, 5, 9, 12, 14) where the geological  
489 characterization indicates DNAPL would migrate if leaked from the PCE tank. In the central part of  
490 the area (MIP3, 6, 7) a combination of the two contaminant profiles was observed.

#### 491 *NAPL FLUTe*

492 A NAPL FLUTe was installed adjacent to each of the three boreholes (CT1-3) where the highest  
493 concentrations of chlorinated solvents were detected and the presence of DNAPL was confirmed by  
494 hydrophobic dye tests. In CT1 and CT3 direct evidence of DNAPL was found around 0.5 m bgs (cf.  
495 Fig. 4). The presence of DNAPL at this depth was confirmed by staining in CTF1, while a  
496 significant smearing of the colored lines was observed in CTF3 (cf. Fig. 5).

497 In CT2, direct evidence of DNAPL was repeatedly found at 2-7.5 m bgs (Fig. 4). At the depths  
498 with the highest DNAPL saturation (2-4 m bgs), staining was found in CTF2 (Fig. 5). At this depth  
499 interval, the average DNAPL saturation was 2.9 % of the total porosity, which indicates that mobile  
500 DNAPL is present in the fractures at this DNAPL saturation. Contact between the NAPL FLUTe  
501 and mobile DNAPL in hydraulically active horizontal fractures is thereby very likely at these  
502 depths. At greater depths, where the DNAPL saturation was below 2.5 % of the total porosity, the  
503 adjacent NAPL FLUTe liner showed slightly more visible colored lines, but no staining was

504 observed. The NAPL FLUTe thereby gives the impression that less DNAPL is present compared to  
505 the subsampling of cores at the adjacent location.

506 The NAPL FLUTe liner is a good tool for direct determination of DNAPL in the borehole.  
507 However, the presence of nearby DNAPL without direct contact to the borehole wall will not be  
508 detected. Concerns that the presence of residual DNAPL may be overlooked in the staining  
509 interpretation have previously been raised (Griffin & Watson, 2002). The nearby location of  
510 residual DNAPL may be indicated by the increased visibility of the colored lines. In initial  
511 laboratory studies (Beyer, 2012), it was found that high dissolved concentrations of chlorinated  
512 solvents would indeed increase the visibility of the colored lines. An aqueous solution saturated  
513 with both PCE and TCE would produce this effect, while a solution saturated only with PCE would  
514 not. Unfortunately, the effect will be difficult to interpret and does not give direct evidence of  
515 DNAPL.

#### 516 *FACT FLUTe*

517 The FACT was employed to better delineate the concentrations over depth; direct contact with the  
518 DNAPL is not needed. The measured concentrations of PCE and TCE on the FACT are generally in  
519 good accordance with the observed staining/coloration trend on the NAPL FLUTe liner (cf. Fig. 5).  
520 In CTF1 and CTF3 the highest concentrations on the FACT are measured at 0.4-0.6 m bgs, where  
521 staining (CTF1) or smearing (CTF3) of the NAPL FLUTe liner is observed and DNAPL is directly  
522 observed in the adjacent core samples (cf. Fig. 4).

523 Interestingly, while DNAPL saturations (~1.5 %) in the adjacent core samples at a depth of  
524 around 0.5 m bgs are comparable for the two locations, the staining on the NAPL FLUTe and the  
525 PCE concentration on the FACT were very different (4 times higher in CTF3). The higher FACT  
526 concentrations in CTF3 are likely a result of the less saturated conditions; at 0.5 m bgs the FACT  
527 had water saturations of around 60 % and 30 % in CTF1 and CTF3, respectively. Preliminary  
528 laboratory results indicated more extensive sorption on the FACT in saturated air than saturated  
529 water (Beyer, 2012) as the diffusion coefficient of PCE in air is four orders of magnitude higher

530 than in water (Mendoza et al., 1996). Hence, the concentrations in the clay till and on the FACT  
531 cannot be directly correlated under variable saturation conditions (cf. Fig. S8).

532 Greatly elevated PCE concentrations were observed on the FACT in CTF2 at 2.0-4.5 m bgs,  
533 which correlates well with the depths where staining on the NAPL FLUTE liner was repeatedly  
534 observed (Fig. 5) and the depths where the DNAPL saturations in the adjacent core samples were  
535 high (Fig. 4). At greater depths (4.8-6.4 m bgs), somewhat elevated PCE concentrations were  
536 observed on the FACT, which correlates to the slightly more visible colored lines that were  
537 observed on the liner (Fig. 5) and DNAPL saturations in the adjacent core samples were in the  
538 residual groupings (Fig. 4). The TCE concentrations on the FACT in CTF2 were generally lower  
539 than in the two other liner boreholes, which is consistent with a lower molar fraction of TCE in the  
540 deeper contamination as observed in the intact coring.

541 The water saturation of the FACT varied significantly over depth and between the boreholes (Fig.  
542 5). The average water saturation of the FACT in the three boreholes was 26 % ( $\sigma = 21$  %), 37 % ( $\sigma$   
543 = 19 %) and 10 % ( $\sigma = 7$  %) for CTF1, CTF2 and CTF3 respectively. In comparison, the saturation  
544 of the less porous clay till formation was around 90 %, which correspond to a saturation of around  
545 25 % given a porosity of 0.97 (FACT) instead of 0.27 (formation). In general, the water saturation  
546 of the FACT can be linked to observation of staining on the NAPL FLUTE and to some degree the  
547 DNAPL saturation in the adjacent cores. The linkage is most visible in CTF1, where the baseline  
548 water saturation on the FACT was around 13 % and six significant peaks of higher water saturation  
549 were observed. Four of the five largest peaks (>40 % saturation) correspond to the four  
550 observations of staining on the NAPL FLUTE, which may correlate to the presence of significant  
551 hydraulically active fractures where DNAPL can be transported. These peaks are also relatively  
552 well correlated to the depths with the highest FID responses in the adjacent MIP7. Very local  
553 occurrence of DNAPL in single fractures is in good accordance with the nature of DNAPL  
554 observations in the adjacent CT1 cores, where only one of the three single point observations of

555 chlorinated solvents above the DNAPL threshold concentration could be confirmed by adjacent  
556 Sudan IV test (5-10 cm spacing).

557 In CTF2, the baseline water saturation is similar to CTF1 in the upper 2 m, but no peaks in water  
558 saturation were observed; no staining on the NAPL FLUTE or DNAPL saturation in the adjacent  
559 cores was observed in these upper 2 m. Deeper than 2 m bgs, the baseline water saturation on the  
560 FACT is higher than in the other two locations (around 27 %), indicating a more water conducting  
561 area. At depths below 2 m bgs, varying degrees of staining on the NAPL FLUTE and DNAPL  
562 detection in the adjacent cores were observed. At 2.5-4.0 m bgs, several closely spaced peaks in the  
563 water saturation (>60 %) were observed; those depths correlate well with the observation of  
564 staining on the NAPL FLUTE and the highest DNAPL saturations (>3 %) in the adjacent cores.  
565 This may indicate a locally more fractured area in the clay till with better possibility of DNAPL  
566 migration. Below 4 m bgs, the lack of saturation peaks indicates a less fractured area without  
567 horizontal DNAPL migration. The FACT concentrations were still somewhat elevated, while no  
568 staining was observed on the NAPL FLUTE, with only a slightly increased visibility of the colored  
569 lines. Around 4.5 m bgs, the DNAPL saturation in the adjacent cores became lower (<2.5 %),  
570 whereby the FACT concentrations likely originated from dissolution of nearby residual DNAPL.

571 In CTF3 the water saturation was generally low without a stable baseline saturation; an increase in  
572 the water saturation was observed around the redox boundary at 4-5 m bgs. The highest water  
573 saturation (30 %) was found around 0.5 m bgs, which was also the location with most visible  
574 staining on the NAPL FLUTE and the only observation of DNAPL in the adjacent cores. This may  
575 indicate an area with relatively few fractures and a greater importance of pore air diffusion in the  
576 matrix.

577 Although the method only adds qualitative data, the FACT has been valuable for improving the  
578 conceptual understanding of DNAPL distribution and mobility in the clay till, which is important  
579 for the aquitard integrity assessment. The trends in concentrations on the FACT are generally in  
580 good overall accordance with the staining on the NAPL FLUTE liner and the DNAPL saturation in

the adjacent core samples. The variable saturation conditions are seen as a main challenge with regard to linking the FACT concentrations to possible DNAPL presence. Modeling has recently been used for improved interpretation of FACT concentrations under saturated aquifer conditions (Broholm et al., 2016). For clay till aquitards with more uniform saturation conditions (i.e. below the water table) it may also be possible to better correlate contaminant concentrations in the formation and on the FACT.

#### *Soil gas survey of natural occurring partitioning tracer ( $Rn^{222}$ )*

The soil gas survey (radon and chlorinated solvents) was challenged by the high back pressure in the dense clay till deposits, whereby the attempted vertical delineation was not possible. The most useful results were achieved from the shallow sampling points (<1.5 m bgs), where soil gases accumulated in the fill below the asphalt capping and samples were retrieved relatively easy.

The results for the source area (PL102, PL105 and PL106) show high PID measurements (>5000 ppm) and relatively high concentrations of chlorinated solvents in the soil gases indicating the presence of DNAPL (cf. Table 2). The relative soil gas concentration of TCE was especially high in the eastern part the source area (PL105), which is consistent with surface spillage of chlorinated solvents during handling in that area compared to subsurface leakage of PCE in the western part of the source area. The results from outside the source area (PL100 and PL101) show relatively low PID measurements (<100 ppm) and relatively low concentrations of chlorinated solvents in the soil gases.

600

**Table 2.** Soil gas survey for chlorinated solvents and  $Rn^{222}$  in shallow sampling points (<1.5 m bgs).

Location	Depth (m bgs)	Back pressure (mbar)	PID (ppm)	PCE (mg/m <sup>3</sup> )	TCE (mg/m <sup>3</sup> )	cis-1,2- DCE (mg/m <sup>3</sup> )	$Rn^{222}$ (kBq/m <sup>3</sup> )
PL100	1.3-1.5	500	61	260	30	0.49	130
PL101	0.3-1.5	350	2.5	38	0.88	0.45	17
PL102 <sup>1</sup>	1.1-1.2	450	5600	830000	5100	8.6	90
PL105 <sup>2</sup>	1.0-1.1	<50	7100	200000	25000	67	30
PL106 <sup>2</sup>	0.9-1.0	100	>10000	1600000	6800	<0.01	220

The chlorinated solvent concentrations are only used qualitatively to indicate likely DNAPL presence in areas where DNAPL has been confirmed by other methods. <sup>1</sup>Strong indirect indication of DNAPL in the area. <sup>2</sup>Direct observation of DNAPL in area.

602

603 With the presence of DNAPL in the source area, the  $Rn^{222}$  measurements should be lower  
 604 compared to the natural background concentrations by partitioning into the DNAPL. However, the  
 605 natural variation in  $Rn^{222}$  is high for the clay till (17-130 kBq/m<sup>3</sup>), whereby the  $Rn^{222}$  concentrations  
 606 in the DNAPL source area (30-220 kBq/m<sup>3</sup>) are not statistically lower than the background levels.

607 Based on the combination of poor sampling conditions for soil gas in the dense clay till deposits  
 608 and the apparent high natural variation in the  $Rn^{222}$  in the heterogeneous clay till deposits, the use of  
 609  $Rn^{222}$  as a partitioning tracer is not recommended for assessment of DNAPL distribution in clay till.

#### 610 *Method performance and recommendations*

611 Based on the performance of the characterization methods (Table 3), the following lines of  
 612 evidence approach is suggested to build conceptual understanding at a fractured clay till site. Initial  
 613 screening by MIP-FID (with GCMS) is done to assist delineation of the DNAPL area and to select  
 614 locations for in-depth characterization with intact coring and subsequent installation of NAPL  
 615 FLUTe (with FACT) in the same borehole. Core sub-sampling is done for quantification of  
 616 contaminant (and DNAPL saturation estimates) and direct evidence of DNAPL by Sudan IV  
 617 hydrophobic dye test (discretization based on PID screening and fracture locations). The NAPL  
 618 FLUTe is used for direct (continuous) evidence of DNAPL and FACT FLUTe sub-sampling for  
 619 water content (unsaturated zone) and relative vertical contaminant distribution.

621 **Table 3.** Performance of the characterization tools and recommendations for use at fractured clay till DNAPL sites.

Method	Performance	Recommendation
Intact cores: Concentrations/DNAPL saturation	Good performance. Good core recovery possible in clay till.	Recommended for quantification of the contaminants (with DNAPL threshold concentrations) and estimation of DNAPL saturation (dependent on the uncertainty of site specific parameters).
Hydrophobic dye test: Sudan IV	Good performance. No false positive DNAPL responses below the DNAPL threshold concentration. Mixed results at DNAPL saturations of 0-0.5 %.	Recommended for direct (point) evidence of DNAPL in clay till. May overlook low residual DNAPL saturations (<0.5 %).
Indigo Blue spray	Poor performance. No observed color response at locations with confirmed DNAPL.	Not recommended for direct evidence of DNAPL in clay till.
OVA by PID (soil samples)	Low-medium performance. No DNAPL indications at responses <1000 ppm, while strong DNAPL	Useful for screening of e.g. core samples for selection of locations for further discretization.

MIP:	ECD	indication at responses >4000 ppm. Poor performance. Detector overloaded at concentrations below the DNAPL threshold concentration.	Not recommended for DNAPL sites.
	FID	Medium performance. No DNAPL indications at responses <2.5 V, while strong DNAPL indication at responses >5 V.	Robust against detector overload in DNAPL areas. Recommended as a continuous screening tool (combine with GCMS) to roughly delineate the DNAPL area.
FLUTE liners:	NAPL FLUTE	Good performance. Residual DNAPL can be overlooked.	Recommended for direct (continuous) evidence of especially mobile DNAPL in clay till.
	FACT FLUTE	Medium performance. Data are hard to interpret. Adds discrete water saturation data on FACT (especially useful in unsaturated media).	Recommended for building conceptual understanding. Currently not useful for DNAPL detection.
Partitioning tracer:	Natural Rn <sup>222</sup>	Poor performance. No statistical difference for DNAPL presence. High variability in background concentrations and difficult sampling conditions (high back pressure)	Further development needed. Not suitable for clay till as the natural variation of Rn <sup>222</sup> is too high in this geological media.

622

## 623 **DNAPL source zone architecture and aquitard integrity**

624 The data set generated supports a division of the source area into an eastern area with a shallower  
625 DNAPL contamination (PCE and TCE) likely resulting from spillage in connection with surface  
626 handling; and a southwestern area with a deeper DNAPL contamination (primarily PCE) likely  
627 resulting from subsurface leakage from the PCE tank and/or the connection pipe to the tank (cf. Fig.  
628 3). Most of the characterization methods were suitable for determination of the approximate depth  
629 of the contamination. The direct observations of DNAPL presence could only be made by intact  
630 coring and NAPL FLUTE, while both MIP-FID with GCMS (for compounds determination) and  
631 FACT supported the intact coring in assessing whether the contamination was primarily PCE or a  
632 combination of both PCE and TCE.

633 The DNAPL source zone architecture in the eastern area is represented by DNAPL at the interface  
634 between the fill layer and clay till aquitard (direct observations) and likely vertical and horizontal  
635 migration in fractures and/or other high permeability features above the redox boundary in the clay  
636 till (mainly strong indirect indications). The indirect indications of DNAPL in the clay till are found  
637 as single observations of residual DNAPL saturations (< 2.5 %) with some spacing (~1 m) in the

638 intact coring and spotting on the NAPL FLUTE coinciding with high water saturation on the FACT  
639 (conductive fractures), indications which are likely linked to separate fractures (cf. Fig. 4-5). No  
640 indication of DNAPL was observed in the reduced clay till. In the southwestern area, the DNAPL  
641 source zone architecture is represented by deeper DNAPL starting around 2 m bgs (direct  
642 observations). DNAPL migration occurs vertically through fractures in the upper part of the clay till  
643 (direct observations), horizontal migration along fractures and/or other high permeability features  
644 above the redox boundary in the clay till (mainly indirect indications), and at one intact coring  
645 location continued vertical migration through fractures in the reduced clay till to the underlying  
646 aquifer (direct observations). The migration primarily occurs in the southwestern direction from the  
647 PCE tank, which is consistent with the fracture orientation typical for the area (cf. Site geology  
648 section).

649 Based on the results, it is expected that extensive vertical DNAPL migration will occur in the  
650 upper oxidized part of clay till aquitards, where (unsaturated) fractures are most abundant.  
651 Significant horizontal migration will also occur at depths with high densities of horizontal fractures  
652 connected to the vertical fractures (e.g. around or above the redox boundary). For the less fractured  
653 reduced part of clay till aquitards, the vertical (and horizontal) migration will be more limited and  
654 the aquitard integrity to DNAPL migration is largely linked with the thickness of this reduced zone  
655 of the clay till aquitards (cf. Fig S14, SI).

656 At the site, the one location where the aquitard integrity was observed to be compromised is in  
657 good agreement with the geological understanding of high risk areas for extensive fracture systems  
658 throughout the clay till unit. This area is represented by a depression in the redox boundary (cf. Fig.  
659 2), identified by a bulk color change, which is often linked with locally more developed fracture  
660 systems, and the thickness of the reduced clay till is less than 2 m. Based on the FACT FLUTE  
661 water saturation in the compromised location, the clay till appears to be more water conducting  
662 (fractured) than the locations in the eastern part of the source area. The most extensive fracture  
663 system indications coincide with the location of mobile DNAPL saturations ( $> 2.5\%$  encountered at



664 2.5-4.5 m bgs) with residual DNAPL saturations ( $< 2.5\%$ ) in the remaining depths. Hence, the  
665 majority of the DNAPL is accumulated in the more extensively fractured clay till above the redox  
666 boundary, while smaller amounts of DNAPL have been observed to penetrate vertically into the less  
667 fractured reduced clay till and to some extent into the underlying brecciated limestone.

668 The compromised aquitard integrity towards DNAPL is further supported by comparison of the  
669 estimated mass discharge of dissolved PCE ( $\sim 2$  kg/year) from the DNAPL source area (cf. SI)  
670 compared to the mass discharge to the on-going remedial pumping system ( $\sim 100$  kg/year) in the  
671 limestone aquifer at the site. This would indicate that significant amounts of DNAPL have been  
672 discharged to the limestone aquifer.

673 The geological understanding is important for conceptual development. The fractured clay till in  
674 the greater Copenhagen area is relatively well-characterized based on excavations in the area. In  
675 areas without prior characterization of fractures, local excavations or use of outcrops, gravel pits or  
676 similar in the area are highly recommended. For characterization of horizontal fractures (and redox  
677 boundary) intact cores are useful, while the FACT FLUTE may give an indication of water  
678 conductive fractures in the vadose zone.

## 679 **Conclusions**

680 The investigations of the PCE source zone showed that 82 % of the samples from the intact coring  
681 did not contain any DNAPL (PCE was below the threshold concentration); those samples only  
682 comprised 4 % of the total PCE mass. The majority of the PCE source zone mass was found as  
683 mobile DNAPL ( $St > 2.5\%$ ) associated with fractures in the clay till (48 % mass, 2 % occurrence)  
684 or as high residual DNAPL ( $St = 1-2.5\%$ ) in the clay till (38 % mass, 9 % occurrence). Hence, high  
685 resolution site characterization is needed for proper mass estimation and design of remedial actions  
686 in the fractured clay till.

687 No single technique was sufficient for characterization of the DNAPL source zone architecture.  
688 However, insight into the source zone architecture in the clay till aquitard was especially assisted by  
689 the use of MIP as a continuous qualitative initial screening tool combined with NAPL FACT

690 FLUTe and coring with quantitative subsample analysis for establishment of DNAPL threshold  
691 concentrations and Sudan IV colorization tests for positive confirmation of DNAPL presence.  
692 Surface geophysics with ground penetrating radar (GPR) and seismic reflection and refraction  
693 (SRR) combined with geologic information supplemented conceptual understanding of the transport  
694 and distribution of DNAPL in the fill and clayey till.

695 The data set generated from the combined use of the various characterization tools supports the  
696 hypothesis that DNAPL released at fractured clay till sites migrated vertically through fractures in  
697 the upper oxidized part of the clay till aquitard, horizontally along fractures and/or other high  
698 permeability features around the redox boundary, and to some extent vertically through the fractures  
699 in the reduced part of the clay till aquitard to the underlying aquifer.

700 The integrity of clay till aquitards to DNAPL migration is linked with the thickness of the less  
701 fractured reduced zone. The vertical migration of DNAPL through the reduced aquitard was only  
702 observed where the reduced clay till is less than 2 m thick, which is consistent with geological  
703 studies on high risk areas for fracture development throughout clay till aquitards. The findings on  
704 clay till aquitard integrity to DNAPL migration are likely transferable to similar primarily oxidized  
705 clay till aquitards of limited thickness.

706

## 707 **Acknowledgements**

708 The presented research was funded by the Capital Region of Denmark through a research  
709 collaboration agreement with DTU Environment on “DNAPL source area characterization  
710 techniques”. The authors acknowledge the assistance with field and laboratory work, analysis, and  
711 graphical assistance by technical staff and students at DTU Environment, especially Bent H. Skov,  
712 Jens S. Sørensen, Lisbet Brusendorff, and Monique Beyer, as well as technical staff and colleagues  
713 from COWI, NIRAS, FLUTe and Probing. We would also like to acknowledge Dr. Knud Erik S.  
714 Klint of the Geological Survey of Denmark and Greenland for support with geological  
715 understanding of the Copenhagen area.

716

## 717 **References**

- 718 Adamson, D.T., Chapman, S., Mahler, N., Newell, C., Parker, B., Pitkin, S., Rossi, M., Singletary,  
719 M. 2014. Membrane Interface Probe Protocol for Contaminants in Low-Permeability Zones.  
720 Groundwater, 52 (4), 550–565.
- 721 Beyer, M. 2012. DNAPL characterization in clayey till & chalk by FACT (FLUTe Activated  
722 Carbon Technique). MSc Thesis, Department of Environmental Engineering, Technical University  
723 of Denmark.
- 724 Broholm, K., Feenstra, S. 1995. Laboratory measurements of the aqueous solubility of mixtures of  
725 chlorinated solvents. Environ. Toxicol. Chem., 14 (1): 9–15.
- 726 Broholm, M.M., Janniche, G.S., Mosthaf, K., Fjordbøge, A.S., Binning, P.J., Christensen, A.G.,  
727 Grosen, B., Jørgensen, T.H., Keller, C., Wealthall, G., Kern-Jespersen, H. 2016. Characterization  
728 of Chlorinated Solvent Contamination in Limestone Using Innovative FLUTe® Technologies in  
729 Combination with Other Methods in a Line of Evidence Approach. J. Contam. Hydrol., 189, 68–85.
- 730 Cherry, J.A., Parker, B., Keller, C. 2007. A new depth-discrete multilevel monitoring approach  
731 for fractured rock. Ground Water Monit. R., 27 (2): 57-70.
- 732 Christiansen, C.M., Riis, C., Christensen, S.B., Broholm, M.M., Christensen, A.G., Klint, K.E.S.,  
733 Wood, J.S.A., Bauer-Gottwein, P., Bjerg, P.L. 2008. Characterization and Quantification of  
734 Pneumatic Fracturing Effects at a Clay Till Site. Environ. Sci. Technol., 42, 570–576.
- 735 Cohen, R.M., Bryda, A.P., Shaw, S.T., Spalding, C.P. 1992. Evaluation of Visual Methods to  
736 Detect NAPL in Soil and Water. Ground Water Monit. R., 12 (4): 132-141.
- 737 D'Affonseca, F.M., Blum, P., Finkel, M., Melzer, R., Grathwohl, P. 2008. Field scale  
738 characterization and modeling of contaminant release from a coal tar source zone. J. Contam.  
739 Hydrol., 102, 120–139.

740 Doherty, R.E., 2000. A history of the production and use of carbon tetrachloride,  
741 tetrachloroethylene, trichloroethylene and 1,1,1-trichloroethane in the United States: Part 1 —  
742 historical background; carbon tetrachloride and tetrachloroethylene. *J. Environ. Forensics* 1, 69–81.

743 Erto, A., Lancia, A., Musmarra, D. 2011. A modelling analysis of PCE/TCE mixture adsorption  
744 based on Ideal Adsorbed Solution Theory. *Sep. Purif. Technol.*, 80, 140-147.

745 Esposito, S.J., Thomson, N.R. 1999. Two-phase flow and transport in a single fracture-porous  
746 medium system. *J. Contam. Hydrol.*, 37, 319–341.

747 Feenstra, S., Mackay, D.M., Cherry, J.A. 1991. A method for assessing residual NAPL based on  
748 organic chemical concentrations in soil samples. *Ground Water Monit. R.* 11, 128–136.

749 Germain, R.W.St., Einarson, M.D., Fure, A., Chapman, S., Parker, B. 2014. Dye based laser-  
750 induced fluorescence sensing of chlorinated solvent DNAPLs. Conference proceedings, paper 1-14,  
751 3<sup>rd</sup> International Symposium on Cone Penetration Testing, May 12-14, 2014, Las Vegas, NV.

752 Griffin, T.W., Watson, K.W. 2002. A Comparison of Field Techniques for Confirming Dense  
753 Nonaqueous Phase Liquids. *Ground Water Monit. R.*, 22(2), 48–59.

754 Hartog, N., Cho, J., Parker, B.L., Annable, M.D. 2010. Characterization of a heterogeneous  
755 DNAPL source zone in the Borden aquifer using partitioning and interfacial tracers: Residual  
756 morphologies and background sorption. *J. Contam. Hydrol.*, 115, 79–89.

757 Höhener, P., Surbeck, H. 2004. Radon-222 as a Tracer for Nonaqueous Phase Liquid in the  
758 Vadose Zone: Experiments and Analytical Model. *Vadose Zone J.*, 3, 1276–1285.

759 Jørgensen, P.R., Broholm, K., Sonnenborg, T.O., Arvin, E. 1998a. DNAPL transport through  
760 macroporous, clayey till columns. *Ground Water*, 36(4), 651–660.

761 Jørgensen, P.R., Hoffmann, M., Kistrup, J.P., Bryde, C., Bossi, R., Villholth, K.G. 2002.  
762 Preferential flow and pesticide transport in a clay-rich till: Field, laboratory, and modeling analysis.  
763 *Water Resour. Res.*, 38 (11): 1246.

764 Jørgensen, P.R., Klint, K.E.S., Kistrup, J.P. 2003. Monitoring Well Interception with Fractures in  
765 Clayey till. *Ground Water*, 41 (6): 772-779.

766 Jørgensen, P.R., McKay, L.D., Spliid, N.H. 1998b. Evaluation of chloride and pesticide transport  
767 in a fractured clayey till using large undisturbed columns and numerical modeling. *Water Resour.*  
768 *Res.*, 34 (4): 539-553.

769 Kjær, K.H., Houmark-Nielsen, M., Richardt, N. 2003. Ice-flow patterns and dispersal of erratics  
770 at the southwestern margin of the last Scandinavian Ice Sheet: signature of palaeo-ice streams.  
771 *Boreas*, 32, 130–148.

772 Klint, K.E.S. 2001. Fractures in glacigene diamict deposits: Origin and distribution. PhD  
773 dissertation, Geological Institute, University of Copenhagen, Denmark.

774 Klint, K.E.S., Nilsson, B., Troldborg, L., Jakobsen, P.R. 2013. A poly morphological landform  
775 approach for hydrogeological applications in heterogeneous glacial sediments. *Hydrogeol. J.*, 21,  
776 1247–1264.

777 Kram, M.L., Lieberman, S.H., Fee, J., Keller, A.A. 2001. Use of LIF for Real-Time In-Situ Mixed  
778 NAPL Source Zone Detection. *Ground Water Monit. R.*, 67-76.

779 Kueper, B.H., McWhorter, D.B. 1991. The Behavior of Dense, Nonaqueous Phase Liquids in  
780 Fractured Clay and Rock. *Ground Water*, 29 (5), 716–728.

781 Lu, C., Bjerg, P.L., Zhang, F., Broholm, M.M. 2011. Sorption of chlorinated solvents and  
782 degradation products on natural clayey tills. *Chemosphere*, 83, 1467–1474.

783 Mackay, D.M., Cherry, J.A., 1989. Groundwater contamination: pump-and-treat remediation.  
784 *Environ. Sci. Technol.*, 23 (6), 630–636.

785 Mariner, P.E., Jin, M., Studer, J.E., Pope, G.A. 1999. The First Vadose Zone Partitioning  
786 Interwell Tracer Test for Nonaqueous Phase Liquid and Water Residual. *Environ. Sci. Technol.*, 33,  
787 2825-2828.

788 McDermott, H.J. 2004. Air Monitoring for Toxic Exposures. 2<sup>nd</sup> ed., John Wiley & Sons, Inc.,  
789 Hoboken, New Jersey.

790 McKay, L.D., Cherry, J.A., Gillham, R.W. 1993. Field Experiments in a Fractured Clay Till. 1.  
791 Hydraulic Conductivity and Fracture Aperture. *Water Resour. Res.*, 29 (4): 1149-1162.

792 Mendoza, C.A., Johnson, R.L., Gillham, R.W. 1996. Vapor Migration in the Vadose Zone. In  
 793 Pankow, J.F., Cherry, J.A. 1996. Dense Chlorinated Solvents and other DNAPLs in Groundwater.  
 794 Waterloo Press, Portland, OR, USA.

795 Mercer, J.W., Cohen, R.M., 1990. A Review of Immiscible Fluids in the Subsurface: Properties,  
 796 Models, Characterization and Remediation. *J. Contam. Hydrol.*, 6, 107–163.

797 O'Hara, S.K., Parker, B.L., Jørgensen, P.R., Cherry, J.A. 2000. Trichloroethene DNAPL flow and  
 798 mass distribution in naturally fractured clay: Evidence of aperture variability. *Water Resour. Res.*,  
 799 36(1), 135–147.

800 Pankow, J.F., Cherry, J.A. 1996. Dense Chlorinated Solvents and other DNAPLs in Groundwater.  
 801 Waterloo Press, Portland, OR, USA.

802 Parker, B.L., Cherry, J.A., Chapman, S.W. 2004. Field study of TCE diffusion profiles below  
 803 DNAPL to assess aquitard integrity. *J. Contam. Hydrol.*, 74, 197–230.

804 Parker, B.L., Cherry, J.A., Chapman, S.W., Guilbeault, M.A. 2003. Review and Analysis of  
 805 Chlorinated Solvent Dense Nonaqueous Phase Liquid Distributions in Five Sandy Aquifers. *Vadose*  
 806 *Zone J.*, 2, 116–137.

807 Parker, B.L., Gillham, R.W., Cherry, J.A. 1994. Diffusive Disappearance of Immiscible-Phase  
 808 Organic Liquids in Fractured Geologic Media. *Ground Water*, 32(5), 805–820.

809 Parker, B.L., McWhorter, D.B., Cherry, J.A. 1997. Diffusive Loss of Non-Aqueous Phase  
 810 Organic Solvents from Idealized Fracture Networks in Geologic Media. *Groundwater*, 35(6), 1077–  
 811 1088.

812 Pitkin, S.E., Cherry, J.A., Ingleton, R.A., Broholm, M. 1999. Field Demonstrations Using the  
 813 Waterloo Ground Water Profiler. *Ground Water Monit. R.*, 19 (2), 122–131.

814 Poulsen, M.M.; Kueper, B.H. 1992. A Field Experiment To Study the Behavior of  
 815 Tetrachloroethylene in Unsaturated Porous Media. *Environ. Sci. Technol.*, 26(5), 889–895.

816 Reynolds, D.A., Kueper, B.H. 2001. Multiphase flow and transport in fractured clay/sand  
 817 sequences. *J. Contam. Hydrol.* 51, 41–62.

818 Reynolds, D.A., Kueper, B.H. 2004. Multiphase flow and transport through fractured  
819 heterogeneous porous media. *J. Contam. Hydrol.* 71, 89–110.

820 Rivett, M.O., Dearden, R.A., Wealthall, G.P. 2014. Architecture, persistence and dissolution of a  
821 20 to 45 year old trichloroethene DNAPL source zone. *J. Contam. Hydrol.*, 170, 95–115.

822 Schubert, M., Paschke, A., Lau, S., Geyer, W., Knöller, K. 2007. Radon as a naturally occurring  
823 tracer for the assessment of residual NAPL contamination of aquifers. *Environ. Pollut.*, 145, 920-  
824 927.

825 Semprini, L., Hopkins, O.S., Tasker, B.R. 2000. Laboratory, Field and Modeling Studies of  
826 Radon-222 as a Natural Tracer for Monitoring NAPL Contamination. *Transport Porous Med.*, 38,  
827 223–240.

828 Slough, K.J.; Sudicky, E.A., Forsyth, P.A. 1999. Numerical simulation of multiphase flow and  
829 phase partitioning in discretely fractured geologic media. *J. Contam. Hydrol.*, 40, 107–136.

830 VanderKwaak, J.E., Sudicky, E.A. 1996. Dissolution of non-aqueous-phase liquids and aqueous-  
831 phase contaminant transport in discretely fractured porous media. *J. Contam. Hydrol.*, 23, 45–68.

832 Winslow, S.D.; Pepich, B.V.; Martin, J.J.; Hallberg, G.R.; Munch, D.J.; Frebis, C.P.; Hedrick,  
833 E.J.; Krop, R.A. 2006. Statistical procedures for determination and verification of minimum  
834 reporting levels for drinking water methods. *Environ. Sci. Technol.*, 40, 281–288.

835 Yang, Z., Niemi, A., Fagerlund, F., Illangasekare, T. 2012. Effects of single-fracture aperture  
836 statistics on entrapment, dissolution and source depletion behavior of dense non-aqueous phase  
837 liquids. *J. Contam. Hydrol.*, 133, 1–16.